Int J Clin Exp Med 2017;10(7):10079-10090
www.ijcem.com /ISSN:1940-5901/IJCEM0047074

Original Article

Mechanism of glycyrrhizin in the treatment of chicken embryo allantoic cavity artery vasospasm

Yong Chen[1], Yongjie Yuan[1], Chao Li[2], Si Yang[3], Jinlu Yu[1]

Departments of [1]Neurosurgery, [2]Neurology, [3]Pediatric Neurology, First Hospital of Jilin University, Changchun, Jilin, China.

Received October 18, 2016; Accepted April 25, 2017; Epub July 15, 2017; Published July 30, 2017

Abstract: To investigate the effects of glycyrrhizin (GL) on chicken embryo allantoic cavity artery (ACA) vasospasm, fresh chicken embryo hatching eggs were selected and randomly divided into a Sham group, a Model group, a Model+0.9% normal saline group (Model+NS), a low-dose GL experimental group (Model+3 μg GL), and a high-dose GL experimental group (Model+6 μg GL). On the 11th day of development, a hemorrhage model was established in the chicken embryos via puncture of the chicken embryo allantois membrane (CAM). On the 5th day after the model was established, the chicken embryos were sacrificed, and pathological sections were observed to determine the influence of different doses of GL on the diameter of the cross-sectional area and the wall thickness of the ACA. In addition, immunoblotting was used to detect changes in oxidative stress-, inflammatory response-, apoptosis- and MAPK pathway-related factors. GL improved the survival rate in the ACA vasospasm model; alleviated ACA vascular spasm (more significantly in the high-dose group); and delayed the decreases in SOD, GR, and CAT expression and the increase in iNOS expression in the ACA. GL also alleviated the increases in IL-6, IL-1β and TNF-α expression; the increase in C-caspase-3 expression and the decrease in Bcl-2 expression; and the increases in p-P38/P38 and p-JNK/JNK expression in the MAPK signaling pathway (more obviously in the high-dose group). Therefore, GL can alleviate the oxidative stress, inflammatory reaction and apoptosis observed in ACA tissue after allantoic cavity hemorrhage, improve the survival rate in the allantoic cavity hemorrhage model in chicken embryos, and improve ACA vasospasm. The alleviation effect of GL on ACA vasospasm after allantoic cavity hemorrhage relies on the influence of the MAPK signaling pathways on p-P38/P38 and p-JNK/JNK protein expression.

Keywords: Allantoic cavity artery (ACA), vasospasm, glycyrrhizin, oxidative stress (OS), inflammation, cell apoptosis

Introduction

Cerebral vasospasm (CVS) after subarachnoid hemorrhage (SAH) is a leading cause of death and disability from aneurysm rupture and bleeding in humans. Although much research has focused on post-SAH CVS, the pathogenesis of CVS remains unclear, and effective treatment measures are lacking [1, 2] because there is no ideal CVS model [3, 4]. This study adopted the previously published allantoic cavity artery (ACA) vasospasm model because the chick embryo ACA vasospasm model can better simulate human post-SAH CVS [5]. Inflammation, oxidative stress (OS) and apoptosis play important roles in the occurrence and development of CVS [6, 7]. This study explored the expression of inflammation in the chicken embryo ACA vasospasm model and the effect of an intervention.

Glycyrrhizin (GL), a major component of the roots of the *Glycyrrhiza* genus, has many effects, including those related to the anti-inflammatory response, resistance to oxidative stress and free radical scavenging [8]. It plays a protective role in ischemic brain injury. GL can significantly reduce the infarction area, improve nerve function and inhibit cerebral edema in a mouse middle cerebral artery occlusion (MCAO) model [9, 10]. The present study demonstrated the remission effects of different doses of GL in the chicken embryo ACA vasospasm model; detected the expression of OS-related proteins, inflammatory response-related factors, apoptosis-related proteins and mitogen-activated pro-

tein kinase (MAPK); and elucidated the related mechanism of GL in the treatment of chicken embryo allantoic cavity ACA vasospasm.

Materials and methods

Experimental animals and grouping

The 120 specific-pathogen-free (SPF) level fresh chicken embryo hatching eggs used in this study, with an average weight of 60.7 ± 3.1 g, were purchased from Beijing Merial-Vital Laboratory Animal Co., Ltd. The eggs were randomly divided into five groups: a Sham group, a Model group, a Model+0.9% normal saline group (Model+NS), a Model+3 μg/g/day GL group (Model+3 μg GL) and a Model+6 μg/g/day GL group (Model+6 μg GL), with 20 eggs in each group. The chick embryos that failed to hatch were excluded and replaced with fertilized eggs from the remainder of the 120 eggs. An automatic incubator was employed to hatch the eggs. The settings of the incubation parameters were as follows: 1-6 days, temperature of 38°C and humidity of 60%; 7-12 days, temperature of 37.8°C and humidity of 55%; and 13-18 days, temperature of 37.6°C and humidity of 60%. The eggs were turned every 90 min. On the 5th day of development, the chicken embryos were observed in a dark room using an egg-candling lamp to remove the chicken embryos that failed to hatch, which were replaced with the spare eggs.

Model establishment

All animal operations were approved by the Ethics Committee of Jilin University. Operations were performed as previously described [5]. Briefly, in the experimental group, 11-day-old chicken embryos were used. The blunt end, or air chamber, was illuminated with a lamp to clearly display the chicken embryo allantois membrane (CAM) blood vessels. One of the CAM blood vessels was selected, and a 16-G syringe needle was used to gently drill a hole in the shell. A 26-G syringe needle was then used to puncture the CAM blood vessels. When obvious bleeding was observed under the egg-candling lamp, the chicken embryo eggs were gently turned to allow the blood to disperse in the allantoic cavity evenly, which prevented the allantoic fluid from becoming cloudy. In the Sham group, the shells of the eggs were drilled with a 16-G syringe needle without puncturing the CAM vein, and the eggs were hatched in the incubator. The egg-candling lamp was used every day to observe the eggs, and dead chicken embryos were eliminated.

Delivery methods

The medications were administered through the air chamber. A needle was inserted at a 45-degree angle from 0.5 cm to 1 cm distal to the edge of the air chamber, and the medications were injected and absorbed via the CAM vessels, which were carefully avoided. The medications were administered immediately after the model was established. The Model+NS group, Model+3 μg/g/day GL group, and Model+6 μg/g/day GL group were administered the same volume (10 μl/g) of a 0.9% saline, 0.3 μg/μl GL saline solution or 0.6 μg/μl GL saline solution, respectively. The above doses were delivered twice daily with an interval of 12 h. The chicken embryo eggs in the Sham and Model groups were not administered any medications and were only illuminated at the blunt end, or air chamber, with the egg-candling lamp. The chicken embryos were defined as surviving if the CAM blood vessels were clearly visible; otherwise, they were defined as dead.

ACA sectioning and H&E staining

Five days after the model was established, the chicken embryos were sacrificed at -80°C for 20 min. Tweezers were first used to open the chicken embryos from the air chamber end, exposing the eggshell membrane at the air chamber end and the closely attached CAM below. The eggshell membrane was wiped with a PBS-dipped swab while the CAM blood vessels at the inner membrane were visible. Larger blood vessels were carefully avoided. A 26-G syringe needle was used to pierce the eggshell membrane and the CAM to reach the allantoic cavity, and as much allantoic fluid as possible was poured out. Then, 4% paraformaldehyde, pre-cooled at 4°C, was injected into the allantoic cavity using a 5 ml syringe. After fixation at 4°C for 2 h, the eggshell was opened and the embryo ventral ACA was observed in the allantoic cavity, which was divided into two branches. Approximately 1 cm of the proximal right branch was collected and fixed in 4% paraformaldehyde for 72 h. Then, it was divided into 3 equal segments, longitudinally embedded in paraffin, and sectioned at 5 μm. The sections

Table 1. The number of dead chicken embryos in each subgroup

	Sham	Model	Model+NS	Model+3 μg GL	Model+6 μg GL
1 day	0	3	2	2	2
2 day	0	2	1	1	1
3 day	0	2	4	1	1
4 day	0	4	3	1	0
5 day	0	1	3	0	0

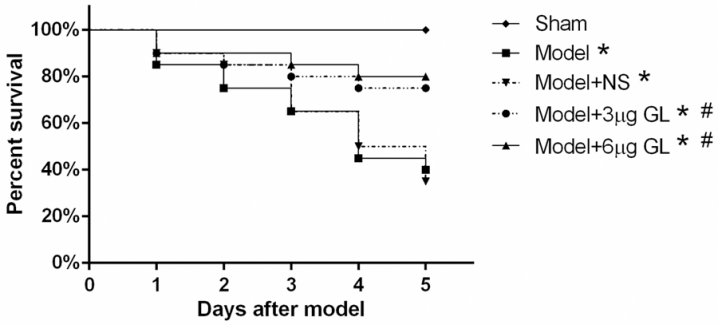

Figure 1. The survival curves for each group of chick embryos. Sham: Sham group; Model: simple model group; Model+NS group: saline control group; Model+3 μg GL: low-dose (3 μg/g/day) glycyrrhizin group; Model+6 μg GL: high-dose (6 μg/g/day) glycyrrhizin group. *P<0.05 vs. Sham, #P<0.05 vs. Model & Model+NS.

were observed and photographed under a microscope after H&E staining.

Measurement of the inner cross-sectional area and wall thickness of the ACA

The inner cross-sectional area of the ACA was measured separately by two technicians using ImageJ in three sections of the ACA (proximal, distal and intermediate segments) after pathological H&E staining. The average inner cross-sectional area of the three ACA sections was taken as the inner cross-sectional area of the ACA, and the average of the values from the two technicians was regarded as the final inner cross-sectional area of the ACA. The wall thickness of the ACA was calculated based on the outer and inner cross-sectional areas of the ACA.

Western blot analysis

The ACA was collected and rinsed with 0.9% saline (containing 0.16 mg/ml heparin) that had been pre-cooled to 4°C. The ACA tissues were sliced, blended in RIPA lysate buffer at 4°C, disrupted via ultrasound, and centrifuged at 4°C. The supernatant was subsequently collected and a BCA kit was used to determine the protein concentration. Then, the proteins were subjected to polyacrylamide gel electrophoresis, with sample loading of 50 μg in each lane. Next, the proteins were transferred to nitrocellulose membranes, which were blocked in 5% skim milk for 1 h and incubated with the appropriate primary antibody at 4°C. Then, the secondary antibody was added, followed by a 1-h incubation at room temperature. The protein bands were developed using ECL developer in a chemiluminescence imager (Sage Creation Science, Beijing).

Statistical analyses

All measurement data are expressed as the mean ± standard deviation. SPSS21.0 was used for the statistical analyses. Analyses of variance were employed to compare the data between multiple sets. The least significant difference (LSD) t-test was used for pairwise comparisons, and the log-rank method was applied for the survival analysis. P<0.05 was considered to indicate a statistically significant difference.

Results

GL improved the survival rate of the chicken embryo ACA vasospasm model

Table 1 and **Figure 1** show the mortality and survival curves for the chicken embryos in each group. On the 5th day after allantoic cavity hemorrhage, the survival rates of the chicken embryos were 0%, 40%, 35%, 75%, and 80% in the Sham, Model, Model+NS, Model+3 μg GL and Model+6 μg GL, respectively. Compared with the mortality in the Sham group, chicken embryo mortality was significantly increased in the Model, Model+NS, Model+3 μg GL and Model+6 μg GL groups (P<0.05). Compared with the mortality in the Model and Model+NS groups, chicken embryo mortality was significantly decreased in the Model+3 μg GL and Model+6 μg GL groups (P<0.05), both of which were GL treatment groups. There were no obvi-

Table 2. Inner cross-sectional area (μm^2) and wall thickness (μm) of the ACA in each group

	Sham	Model	Model+NS	Model+3 μg GL	Model+6 μg GL
Area	144,629.72 ± 2975.94	90,058.93 ± 2063.17*	88,946.58 ± 2103.04*	113,489.50 ± 2648.54$^{*,\#}$	123,109.60 ± 2593.73$^{*,\#,\$}$
Thickness	44.17 ± 1.82	52.94 ± 1.79*	53.02 ± 1.90*	48.38 ± 1.69$^{*,\#}$	46.50 ± 1.83$^{*,\#,\$}$

$^{*}P<0.05$ vs. Sham, $^{\#}P<0.05$ vs. Model & Model+NS, $^{\$}P<0.05$ vs. Model+3 μg GL.

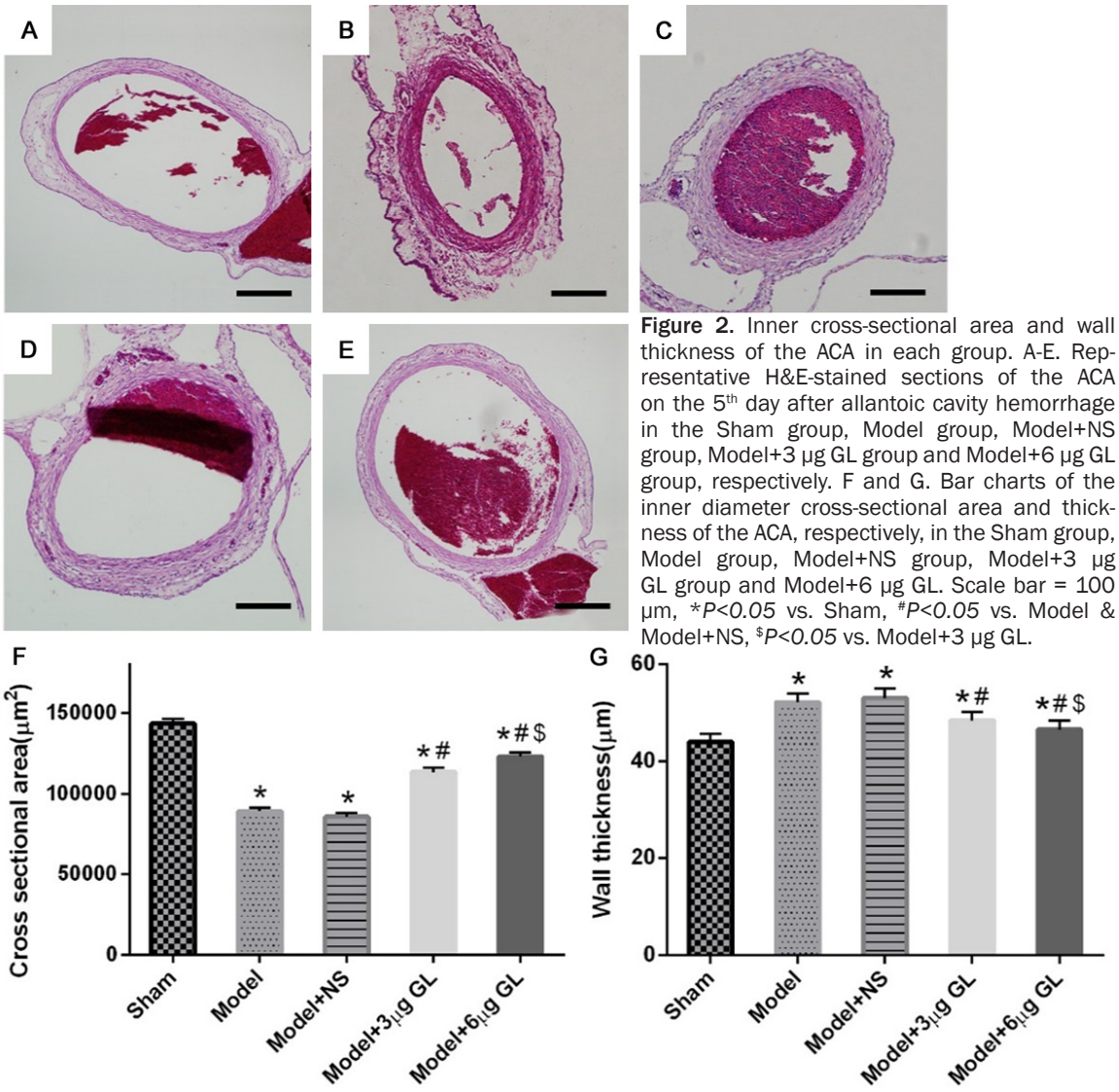

Figure 2. Inner cross-sectional area and wall thickness of the ACA in each group. A-E. Representative H&E-stained sections of the ACA on the 5th day after allantoic cavity hemorrhage in the Sham group, Model group, Model+NS group, Model+3 μg GL group and Model+6 μg GL group, respectively. F and G. Bar charts of the inner diameter cross-sectional area and thickness of the ACA, respectively, in the Sham group, Model group, Model+NS group, Model+3 μg GL group and Model+6 μg GL. Scale bar = 100 μm, $^{*}P<0.05$ vs. Sham, $^{\#}P<0.05$ vs. Model & Model+NS, $^{\$}P<0.05$ vs. Model+3 μg GL.

ous differences between the Model and the Model+NS groups or between the Model+3 μg GL and the Model+6 μg GL groups regarding chicken embryo mortality ($P>0.05$).

GL improved ACA vasospasm after allantoic cavity hemorrhage

Table 2 and **Figure 2** show the inner cross-sectional area and wall thickness of the ACA on the 5th day of allantoic cavity hemorrhage, as determined using typical H&E-stained paraffin sections. Compared with the Sham group, in the Model+NS, Model+3 μg GL and Model+6 μg GL groups, the inner cross-sectional area of the ACA was significantly decreased, whereas the wall thickness of the ACA was obviously increased; these differences were statistically significant ($P<0.05$). The decrease in the inner cross-sectional area of the ACA and the increase in the wall thickness of the ACA were both alleviated in the Model+3 μg GL and Model+6

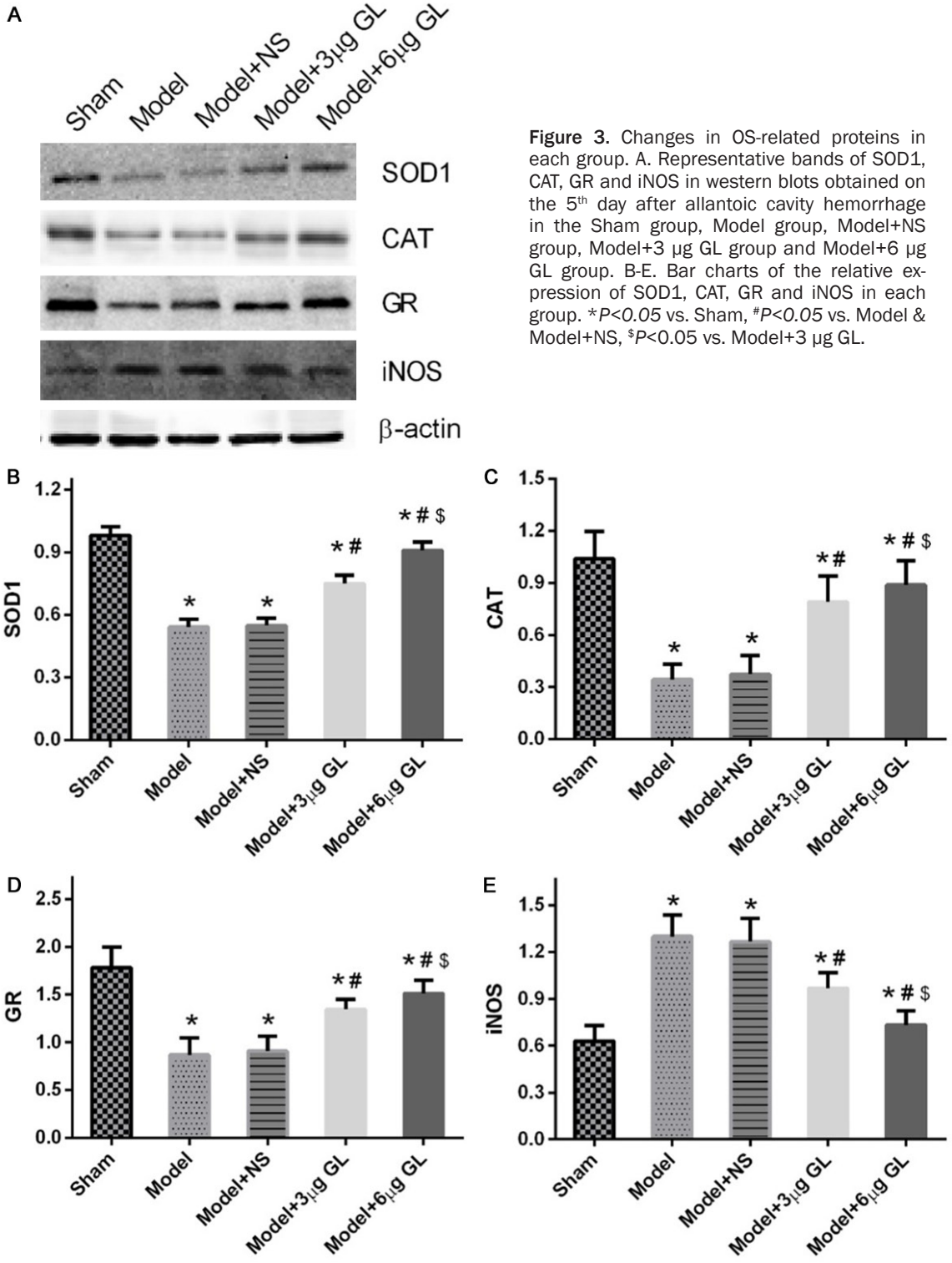

Figure 3. Changes in OS-related proteins in each group. A. Representative bands of SOD1, CAT, GR and iNOS in western blots obtained on the 5th day after allantoic cavity hemorrhage in the Sham group, Model group, Model+NS group, Model+3 μg GL group and Model+6 μg GL group. B-E. Bar charts of the relative expression of SOD1, CAT, GR and iNOS in each group. **P*<0.05 vs. Sham, #*P*<0.05 vs. Model & Model+NS, $*P*<0.05 vs. Model+3 μg GL.

μg GL groups compared with the corresponding parameters in the Model and Model+NS groups (*P*<0.05). Compared with the Model+3 μg GL group, the Model+6 μg GL group showed greater alleviation of the decrease in the inner cross-sectional area of the ACA and the increase in the wall thickness of the ACA; these differences were statistically significant (*P*<0.05). There were no obvious differences between the Model and Model+NS groups in the inner cross-sectional area and wall thickness of the ACA (*P*>0.05).

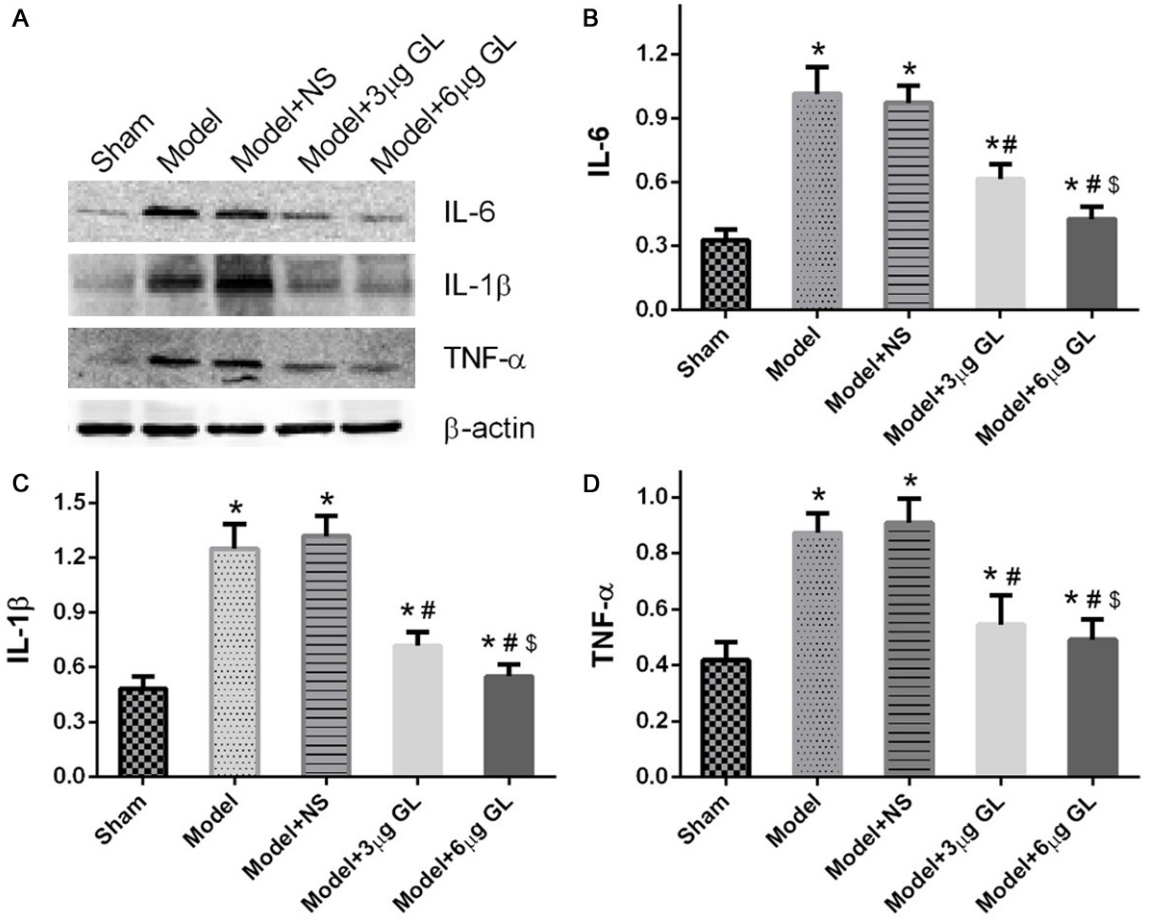

Figure 4. Changes in inflammation-related proteins in each group. A. Representative bands of IL-6, IL-1β, and TNF-α in western blots obtained on the 5th day after allantoic cavity hemorrhage in the Sham group, Model group, Model+NS group, Model+3 μg GL group and Model+6 μg GL group. B-D. Bar charts of the relative expression of IL-6, IL-1β and TNF-α in each group. **P*<0.05 vs. Sham, #*P*<0.05 vs. Model & Model+NS, $*P*<0.05 vs. Model+3 μg GL.

Influence of GL on the expression of OS-related proteins

The western blot results (**Figure 3**) suggested that, on the 5th day of allantoic cavity hemorrhage induced by puncture in chicken embryo CAM blood vessels, the expression of OS-related enzymes such as SOD1, CAT and GR was decreased and the expression of iNOS was significantly elevated in the ACA of the Model, Model+NS, Model+3 μg GL and Model+6 μg GL groups compared with their expression in the Sham group; these differences were statistically significant (*P*<0.05). Compared with the Model and Model+NS groups, the Model+3 μg GL and Model+6 μg GL groups showed decreases in SOD1, CAT and GR expression, and the elevation of iNOS expression was alleviated (*P*<0.05). The degree of alleviation was greater in the Model+6 μg GL group than in the Model+3 μg GL group (*P*<0.05). There were no obvious differences between the Model and Model+NS groups regarding the changes in SOD1, CAT, GR, and iNOS expression in the ACA tissues (*P*>0.05).

Influence of GL on the expression of inflammation-related factors

The western blot results (**Figure 4**) suggested that compared with their expressions in the Sham group, on the 5th day of allantoic cavity hemorrhage, the expressions of inflammation-related proteins such as IL-6, IL-1β and TNF-α were increased in the ACA of the Model, Model+NS, Model+3 μg GL and Model+6 μg GL groups; these differences were statistically significant (*P*<0.05). The increases in IL-6, IL-1β and TNF-α expression were alleviated in the Model+3 μg GL and Model+6 μg GL groups

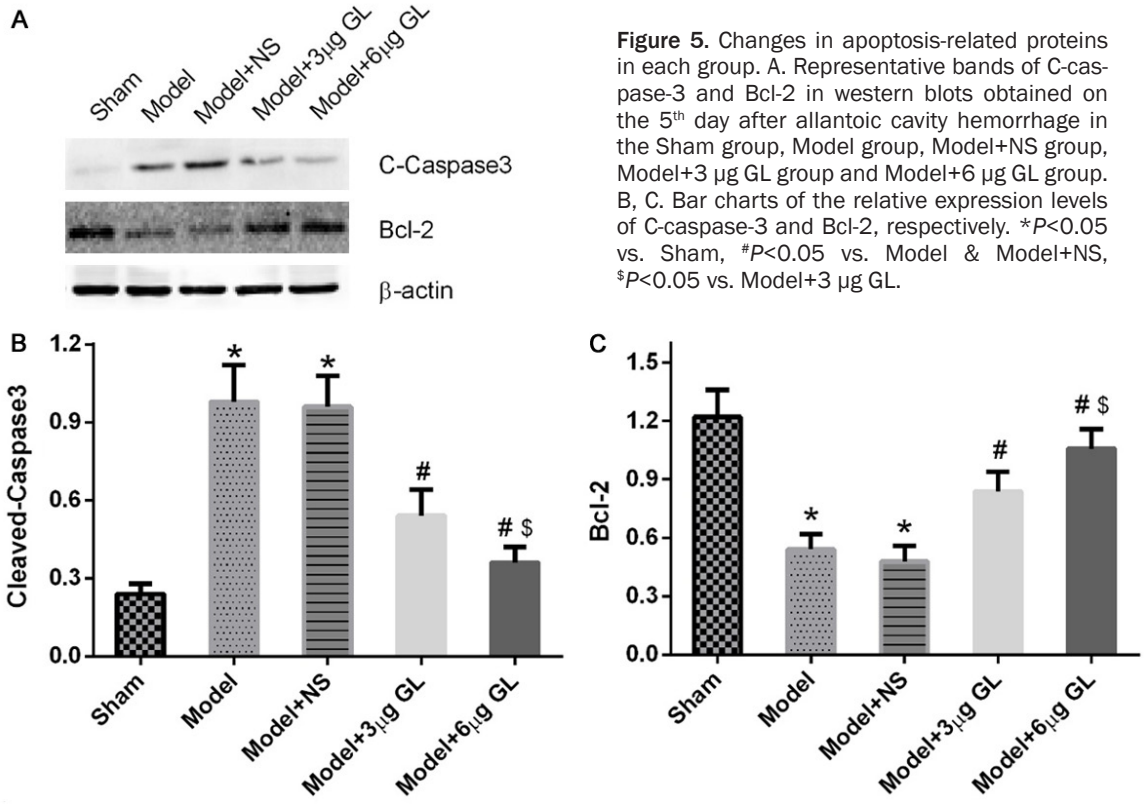

Figure 5. Changes in apoptosis-related proteins in each group. A. Representative bands of C-caspase-3 and Bcl-2 in western blots obtained on the 5th day after allantoic cavity hemorrhage in the Sham group, Model group, Model+NS group, Model+3 μg GL group and Model+6 μg GL group. B, C. Bar charts of the relative expression levels of C-caspase-3 and Bcl-2, respectively. **P*<0.05 vs. Sham, #*P*<0.05 vs. Model & Model+NS, $*P*<0.05 vs. Model+3 μg GL.

compared with those in the Model and Model+NS groups (*P*<0.05). The degree of alleviation was greater in the Model+6 μg GL group than in the Model+3 μg GL group (*P*<0.05). There were no obvious differences between the Model and Model+NS groups in terms of IL-6, IL-1β and TNF-α expression in ACA tissues (*P*>0.05).

Influence of GL on the expression of apoptosis-related proteins

The western blot results (**Figure 5**) suggested that compared with the expression levels observed in the Sham group, on the 5th day of allantoic cavity hemorrhage, the expression of C-caspase-3 was increased andthat of Bcl-2 was significantly decreased in the ACA tissue in the Model, Model+NS, Model+3 μg GL and Model+6 μg GL groups (*P*<0.05). Compared with the Model and Model+NS groups, the increase of C-caspase-3 and the decrease of Bcl-2 were alleviated in the Model+3 μg GL and Model+6 μg GL groups (*P*<0.05). The degree of alleviation was greater in the Model+6 μg GL group than in the Model+3 μg GL group, and this difference was statistically significant (*P*<0.05). There were no obvious differences between the Model and Model+NS group regarding C-caspase-3 and Bcl-2 expression in the ACA tissues (*P*>0.05).

Influence of GL on MAPK pathway-related protein expression

The western blot results (**Figure 6**) suggested that compared with the expression level in the Sham group, on the 5th day of allantoic cavity hemorrhage, the level of MAPK pathway-related protein expression (p-p38/p38, p-JNK/JNK and p-ERK/ERK) was increased in the Model, Model+NS, Model+3 μg GL and Model+6 μg GL groups, and these differences were statistically significant (*P*<0.05). Compared with those in the Model and Model+NS groups, the increases in p-p38/p38 and p-JNK/JNK protein expression were alleviated in the Model+3 μg GL and Model+6 μg GL groups (*P*<0.05). Compared with that in the Model+3 μg GL group, the alleviation of p-p38/p38 and p-JNK/JNK protein expression in the ACA tissues was greater in the Model+6 μg GL group, and these differences were statistically significant (*P*<0.05). There were no obvious differences between the

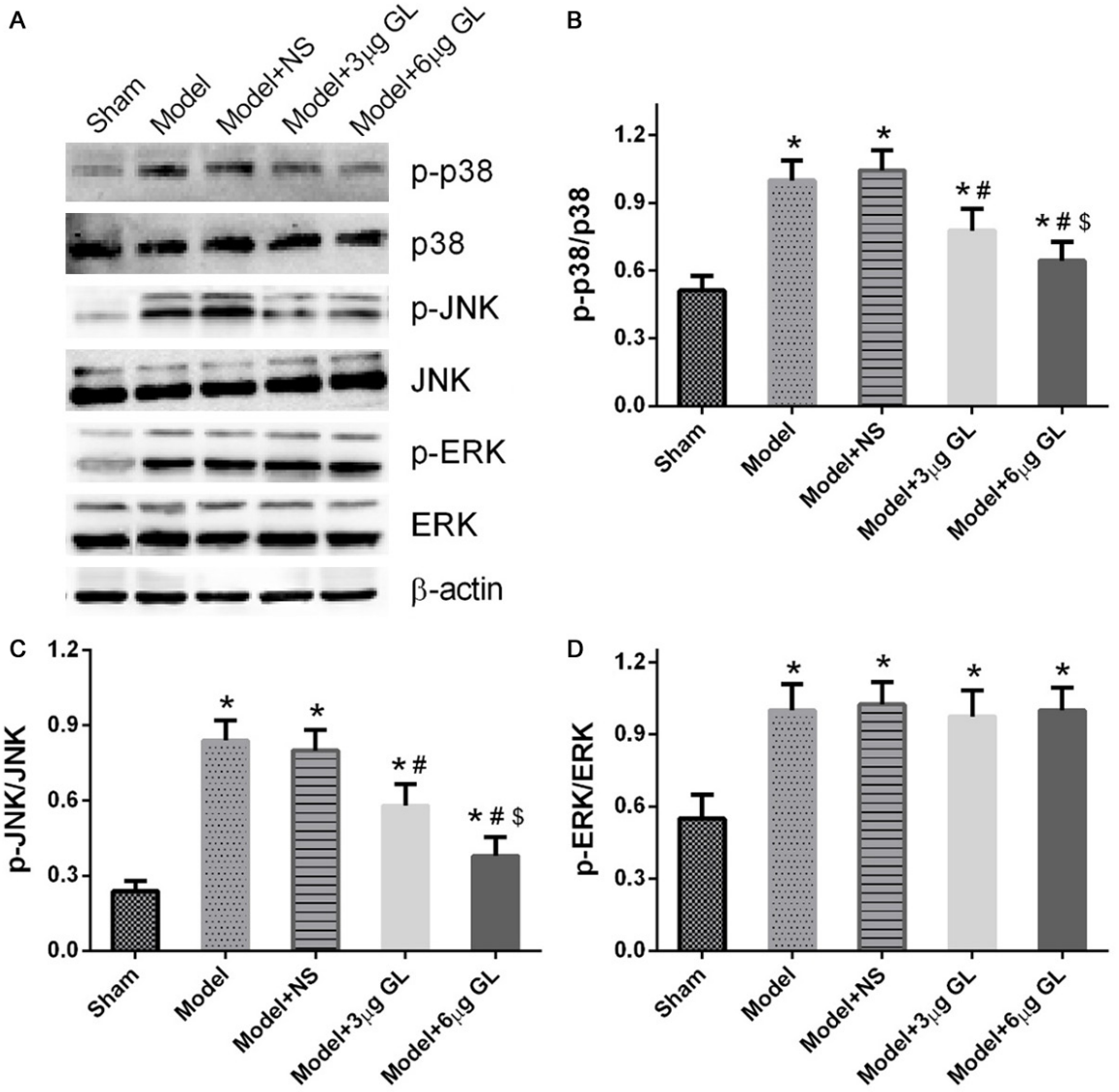

Figure 6. Changes in the protein expression of p-p38/p38, p-JNK/JNK and p-ERK/ERK in each group. A. Representative bands of p-p38/p38, p-JNK/JNK and p-ERK/ERK in western blots obtained on the 5th day after allantoic cavity hemorrhage in the Sham group, Model group, Model+NS group, Model+3 μg GL group and Model+6 μg GL group. B-D. Bar charts of the relative expression of p-p38/p38, p-JNK/JNK and p-ERK/ERK in each group. *$P<0.05$ vs. Sham, #$P<0.05$ vs. Model & Model+NS, $$P<0.05$ vs. Model+3 μg GL.

Model and Model+NS groups in the levels of p-p38/p38 and p-JNK/JNK protein expression in the ACA tissues ($P>0.05$). There were also no obvious differences between the Model, Model+NS, Model+3 μg GL and Model+6 μg GL groups regarding the level of p-ERK/ERK protein expression in the ACA ($P>0.05$).

Discussion

This study adopted the previously established chicken embryo ACA vasospasm model, which simulates post-SAH CVS [5]. Many studies have confirmed that inflammation, oxidative stress and cell apoptosis after SAH play important roles in the occurrence and development of CVS [2, 6, 7, 11-21]. Therefore, this study explored the expression of inflammation in the chicken embryo ACA vasospasm model and the effects of an intervention. In this work, GL was investigated as the intervention. GL, which is a major active constituent extracted from the roots of the licorice genus, has been widely applied in the treatment of chronic viral hepati-

tis and gastric ulcers [8, 22-24]. Studies have revealed that GL exhibits anti-inflammatory, anti-oxidant stress and neural protective effects [8-10, 22, 25, 26]. There are few studies on the effects of GL on post-SAH CVS. Our study showed that oxidative stress, the inflammatory reaction and apoptosis play important roles in the CAM hemorrhage-induced chicken embryo ACA vasospasm model generated via-CAM puncture. Therefore, we used different doses of GL to improve the vasospasm of the chicken embryo ACA, and we discuss the related mechanisms.

Our experiment showed that on the 5th day of allantoic cavity hemorrhage induced by CAM puncture, the chicken embryo mortality rates were 0%, 60%, 65%, 25%, and 20% in the Sham, Model, Model+NS, Model+3 μg GL and Model+6 μg GL groups, respectively. Compared with the mortality in the Sham group, chicken embryo mortality was significantly increased in the Model, Model+NS, Model+3 μg GL and Model+6 μg GL groups. Compared with the mortality in the Model and Model+NS groups, chicken embryo mortality was significantly decreased in the groups receiving the medication (GL), suggesting that GL can reduce the mortality of chicken embryos with allantoic cavity hemorrhage. There was a greater decrease in chicken embryo mortality in the high-dose group than in the low-dose group, but this difference was not statistically significant. Compared with the corresponding parameters in the Sham group, the ACA inner cross-sectional area was obviously decreased and the ACA wall thickness was significantly increased in the Model, Model+NS, Model+3 μg GL and Model+6 μg GL groups. Compared with the Model and Model+NS groups, the Model+3 μg GL and Model+6 μg GL groups showed alleviated ACA vasospasm. In addition, the degree of the decrease in the inner cross-sectional area and the degree of the increase in wall thickness were both significantly alleviated. The degree of alleviation was more obvious in the Model+6 μg GL group than in the Model+3 μg GL group. This suggests that GL can significantly improve the ACA vasospasm of ACA allantoic cavity hemorrhage of the chicken embryo CAM within the dosage range of 3 μg/g/day-6 μg/g/day. The effects became stronger with an increased dosage of the medication, but the ACA vasospasm induced by allantoic cavity hemorrhage could not be completely reversed.

The detection of OS- and inflammation-related factors revealed that compared with the Sham group, the expression of OS-related enzymes such as SOD1, CAT, and GR was obviously decreased in the ACA, whereas iNOS expression was significantly increased. The expression of inflammation-related factors such as IL-6, IL-1β and TNF-α was also markedly elevated in the Model, Model+NS, Model+3 μg GL and Model+6 μg GL groups. Compared with the Model and Model+NS groups, the above changes were obviously alleviated in the Model+3 μg GL and Model+6 μg GL groups. The reduction of SOD1, CAT and GR expression and the increase of iNOS, IL-6, IL-1β and TNF-α were alleviated to a greater extent in the Model+6 μg GL group than in the Model+3 μg GL group. There were no obvious differences between the Model group and Model+NS group regarding the SOD1, CAT, GR, iNOS, IL-6, IL-1β and TNF-α protein expression in the ACA tissues. These results suggested that GL decreased oxidative stress and inflammation in the ACA after allantoic cavity hemorrhage. The effect was greater in the high-dose group; however, the occurrence of inflammation and oxidative stress could not be completely alleviated, which is consistent with the effects of GL in improving the curative effect of ACA vasospasm [25, 26].

An evaluation of the post-SAH CVS animal model confirmed that the number of cerebrovascular cells with positive TUNEL staining was obviously increased; the expression of C-caspase-3, caspase-8, p53 and cytochrome c was significantly increased; and the expression of apoptosis-inhibitory proteins such as Bcl-2, Bcl-xl, and Bcl-x was decreased [27-29]. Our results demonstrated that compared with the expression levels in the Sham group, the expression of C-caspase-3 was obviously increased and that of Bcl-2 was obviously decreased in the Model, Model+NS, Model+3 μg GL and Model+6 μg GL groups. Compared with the Model and Model+NS groups, the above changes were obviously alleviated in the Model+3 μg GL and Model+6 μg GL groups, particularly in the Model+6 μg GL group. There were no obvious differences between the Model and Model+NS groups regarding the protein expression of C-caspase-3 and Bcl-2 in the ACA, suggesting that GL can reduce cell apoptosis in the ACA after allantoic cavity hemorrhage.

Three subgroups (JNK, p38 and ERK) of MAPKs are the most widely investigated in post-SAH CVS studies and are considered to play important roles in the occurrence and development of CVS [30-32]. Our results showed that compared with the levels in the Sham group, on the 5th day of chicken embryo allantoic cavity hemorrhage, the p-p38/p38, p-JNK/JNK and p-ERK/ERK levels were significantly increased in the Model, Model+NS, Model+3 μg GL and Model+6 μg GL groups. Compared with the levels in the Model and Model+NS groups, the increases in the levels of p-p38/p38 and p-JNK/JNK were significantly alleviated in the Model+3 μg GL and Model+6 μg GL groups, whereas there were no obvious changes in the proportion of p-ERK/ERK protein expression. Furthermore, there were no obvious differences between the Model and Model+NS groups in the levels of p-p38/p38, p-JNK/JNK and p-ERK/ERK in the ACA. These results suggested that chicken embryo allantoic cavity hemorrhage could induce up-regulated expression of p-p38/p38, p-JNK/JNK and p-ERK/ERK in the MAPK pathways, which could be alleviated by GL, and that the effect in the high-dose group was obvious. In this experiment, GL likely exerted anti-oxidative stress, anti-inflammation and anti-apoptosis effects and thereby alleviated allantoic cavity hemorrhage-induced ACA vasospasm by reducing the levels of p-p38/p38 and p-JNK/JNK, decreasing the expression of iNOS, IL-6, IL-1β, TNF-α and C-caspase-3, and increasing the expression of SOD1, CAT, GR and Bcl-2. However, GL cannot reduce the ratio of p-ERK/ERK expression, possibly because GL does not completely reverse the ACA vasospasm induced by allantoic cavity hemorrhage.

Therefore, GL can reduce the high mortality of the allantoic cavity hemorrhage model induced in chicken embryo CAM vessels due to its anti-oxidation, anti-inflammatory and embryonic cell protection properties, which effectively relieves the ACA vasospasm caused by allantoic cavity hemorrhage; alleviates the degree of the decreases in SOD1, CAT and GR; reduces the increases in the expression of iNOS, IL-6, IL-1β and TNF-α; and alleviates the increase in C-caspase-3 and decrease in Bcl-2. The changes were more significant in the high-dose group. GL may also exert anti-oxidative stress, anti-inflammation and anti-apoptosis effects by reducing the levels of p-p38/p38 and p-JNK/JNK protein expression.

Acknowledgements

This work was supported by the National Natural Science Foundation of China (81200888).

Disclosure of conflict of interest

None.

Address correspondence to: Jinlu Yu, Department of Neurosurgery, The First Hospital of Jilin University, 71 Xinmin Avenue, Changchun 130021, Jilin, China. E-mail: jlyu@jlu.edu.cn

References

[1] Serrone JC, Maekawa H, Tjahjadi M and Hernesniemi J. Aneurysmal subarachnoid hemorrhage: pathobiology, current treatment and future directions. Expert Rev Neurother 2015; 15: 367-380.

[2] Zhou Y, Martin RD and Zhang JH. Advances in experimental subarachnoid hemorrhage. Acta Neurochir Suppl 2011; 110: 15-21.

[3] Fathi AR, Bakhtian KD, Marbacher S, Fandino J and Pluta RM. Blood clot placement model of subarachnoid hemorrhage in non-human primates. Acta Neurochir Suppl 2015; 120: 343-346.

[4] Muroi C, Fujioka M, Okuchi K, Fandino J, Keller E, Sakamoto Y, Mishima K, Iwasaki K and Fujiwara M. Filament perforation model for mouse subarachnoid hemorrhage: surgical-technical considerations. Br J Neurosurg 2014; 28: 722-732.

[5] Yuan Y, Xu K, Wu W, Luo Q, Yu J. Application of the chick embryo chorioallantoic membrane in neurosurgery disease. Int J Med Sci 2014; 11: 1275-1281.

[6] Mori T, Nagata K, Town T, Tan J, Matsui T and Asano T. Intracisternal increase of superoxide anion production in a canine subarachnoid hemorrhage model. Stroke 2001; 32: 636-642.

[7] Kaneda K, Fujita M, Yamashita S, Kaneko T, Kawamura Y, Izumi T, Tsuruta R, Kasaoka S and Maekawa T. Prognostic value of biochemical markers of brain damage and oxidative stress in post-surgical aneurysmal subarachnoid hemorrhage patients. Brain Res Bull 2010; 81: 173-177.

[8] Chang CZ, Wu SC and Kwan AL. Glycyrrhizin attenuates proinflammatory cytokines through a peroxisome proliferator-activated receptor-gamma-dependent mechanism and experimental vasospasm in a rat model. J Vasc Res 2015; 52: 12-21.

[9] Gong G, Xiang L, Yuan L, Hu L, Wu W, Cai L, Yin L and Dong H. Protective effect of glycyrrhizin,

a direct HMGB1 inhibitor, on focal cerebral ischemia/reperfusion-induced inflammation, oxidative stress, and apoptosis in rats. PLoS One 2014; 9: e89450.
[10] Haleagrahara N, Varkkey J and Chakravarthi S. Cardioprotective effects of glycyrrhizic acid against isoproterenol-induced myocardial ischemia in rats. Int J Mol Sci 2011; 12: 7100-7113.
[11] Matz PG, Copin JC and Chan PH. Cell death after exposure to subarachnoid hemolysate correlates inversely with expression of CuZn-superoxide dismutase. Stroke 2000; 31: 2450-2459.
[12] Watanabe T, Sasaki T, Asano T, Takakura K, Sano K, Fuchinoue T, Watanabe K, Yoshimura S and Abe K. Changes in glutathione peroxidase and lipid peroxides in cerebrospinal fluid and serum after subarachnoid hemorrhage--with special reference to the occurrence of cerebral vasospasm. Neurol Med Chir (Tokyo) 1988; 28: 645-649.
[13] Kamii H, Kato I, Kinouchi H, Chan PH, Epstein CJ, Akabane A, Okamoto H and Yoshimoto T. Amelioration of vasospasm after subarachnoid hemorrhage in transgenic mice overexpressing CuZn-superoxide dismutase. Stroke 1999; 30: 867-71; discussion 872.
[14] Macdonald RL, Weir BK, Runzer TD, Grace MG and Poznansky MJ. Effect of intrathecal superoxide dismutase and catalase on oxyhemoglobin-induced vasospasm in monkeys. Neurosurgery 1992; 30: 529-539.
[15] Sabri M, Ai J, Knight B, Tariq A, Jeon H, Shang X, Marsden PA and Macdonald RL. Uncoupling of endothelial nitric oxide synthase after experimental subarachnoid hemorrhage. J Cereb Blood Flow Metab 2011; 31: 190-199.
[16] Sabri M, Ai J, Lass E, D'abbondanza J and Macdonald RL. Genetic elimination of eNOS reduces secondary complications of experimental subarachnoid hemorrhage. J Cereb Blood Flow Metab 2013; 33: 1008-1014.
[17] Rodríguez-Rodríguez A, Egea-Guerrero JJ, Ruiz de Azúa-López Z and Murillo-Cabezas F. Biomarkers of vasospasm development and outcome in aneurysmal subarachnoid hemorrhage. J Neurol Sci 2014; 341: 119-127.
[18] Przybycien-Szymanska MM and Ashley WW Jr. Biomarker discovery in cerebral vasospasm after aneurysmal subarachnoid hemorrhage. J Stroke Cerebrovasc Dis 2015; 24: 1453-1464.
[19] Bowman G, Dixit S, Bonneau RH, Chinchilli VM and Cockroft KM. Neutralizing antibody against interleukin-6 attenuates posthemorrhagic vasospasm in the rat femoral artery model. Neurosurgery 2004; 54: 719-25; discussion 725.
[20] Jedrzejowska-Szypułka H, Larysz-Brysz M, Kukla M, Snietura M and Lewin-Kowalik J. Neutralization of interleukin-1β reduces vasospasm and alters cerebral blood vessel density following experimental subarachnoid hemorrhage in rats. Curr Neurovasc Res 2009; 6: 95-103.
[21] Vecchione C, Frati A, Di Pardo A, Cifelli G, Carnevale D, Gentile MT, Carangi R, Landolfi A, Carullo P, Bettarini U, Antenucci G, Mascio G, Busceti CL, Notte A, Maffei A, Cantore GP and Lembo G. Tumor necrosis factor-α mediates hemolysis-induced vasoconstriction and the cerebral vasospasm evoked by subarachnoid hemorrhage. Hypertension 2009; 54: 150-156.
[22] Michaelis M, Geiler J, Naczk P, Sithisarn P, Leutz A, Doerr HW and Cinatl J Jr. Glycyrrhizin exerts antioxidative effects in H5N1 influenza a virus-infected cells and inhibits virus replication and pro-inflammatory gene expression. PLoS One 2011; 6: e19705.
[23] Yoshida T, Abe K, Ikeda T, Matsushita T, Wake K, Sato T, Sato T and Inoue H. Inhibitory effect of glycyrrhizin on lipopolysaccharide and d-galactosamine-induced mouse liver injury. Eur J Pharmacol 2007; 576: 136-142.
[24] Yoshida T, Kobayashi M, Li XD, Pollard RB and Suzuki F. Inhibitory effect of glycyrrhizin on the neutrophil-dependent increase of R5 HIV replication in cultures of macrophages. Immunol Cell Biol 2009; 87: 554-558.
[25] Kim SW, Jin Y, Shin JH, Kim ID, Lee HK, Park S, Han PL and Lee JK. Glycyrrhizic acid affords robust neuroprotection in the postischemic brain via anti-inflammatory effect by inhibiting HMGB1 phosphorylation and secretion. Neurobiol Dis 2012; 46: 147-156.
[26] Hou SZ, Li Y, Zhu XL, Wang ZY, Wang X and Xu Y. Ameliorative effects of diammonium glycyrrhizinate on inflammation in focal cerebral ischemic-reperfusion injury. Brain Res 2012; 1447: 20-27.
[27] Cheng G, Wei L, Zhi-Dan S, Shi-Guang Z and Xiang-Zhen L. Atorvastatin ameliorates cerebral vasospasm and early brain injury after subarachnoid hemorrhage and inhibits caspase-dependent apoptosis pathway. BMC Neurosci 2009; 10: 7.
[28] Gao C, Liu X, Liu W, Shi H, Zhao Z, Chen H and Zhao S. Anti-apoptotic and neuroprotective effects of tetramethylpyrazine following subarachnoid hemorrhage in rats. Auton Neurosci 2008; 141: 22-30.
[29] Kooijman E, Nijboer CH, van Velthoven CT, Kavelaars A, Kesecioglu J and Heijnen CJ. The rodent endovascular puncture model of subarachnoid hemorrhage: mechanisms of brain damage and therapeutic strategies. J Neuroinflammation 2014; 11: 2.
[30] Suzuki H, Hasegawa Y, Kanamaru K and Zhang JH. Mitogen-activated protein kinases in cere-

bral vasospasm after subarachnoid hemorrhage: a review. Acta Neurochir Suppl 2011; 110: 133-139.

[31] Laher I and Zhang JH. Protein kinase C and cerebral vasospasm. J Cereb Blood Flow Metab 2001; 21: 887-906.

[32] Aoki K, Zubkov AY, Tibbs RE and Zhang JH. Role of MAPK in chronic cerebral vasospasm. Life Sci 2002; 70: 1901-1908.